ELECTRICAL PROPERTIES OF DENDRITIC SPINES WITH BULBOUS END TERMINALS

MITSUO KAWATO
Department of Biophysical Engineering, Faculty of Engineering Science, Osaka University, Osaka, Japan

NAKAAKIRA TSUKAHARA
Department of Biophysical Engineering, Faculty of Engineering Science, Osaka University, Osaka, Japan and National Institute for Physiological Sciences, Myodaiji, Japan

ABSTRACT Several suggestions have been made about the functional significance of dendritic spines in connection with synaptic plasticity. We investigated transient electrical behavior of spines with bulbous terminals in neurons with arbitrary dendritic geometries. It is shown that postsynaptic potential transform caused by a synapse on a spine can be resolved into a product of two transfer functions and the synaptic input current transform. The first transfer function was determined to be independent of the spine. The second transfer function represents the straightforward attenuation effect of the spine, which determines the effective synaptic current reaching the parent dendrite. Using what is known of the size and the shape of spines from histology, we conclude that almost all of the synaptic current flow into the parent dendrite, and that therefore the straightforward attenuation effect is negligible. Consequently, when the synaptic current remained unaltered, as was the case for a large synaptic resistance as compared with the spine stem resistance, a morphological change of the spine did not produce an effective change in the postsynaptic potential. On the other hand, when the synaptic resistance is compared with the spine stem impedance, the morphological change of the spine might induce changes of the synaptic current and the postsynaptic potential.

INTRODUCTION

Many synapses in the brain are situated on dendritic spines. Dendritic spines show considerable variation in size and shape. Peters and Kaiserman-Abramof (1970) classified spines into the following three types. The most common (72%) have long, thin stalks and small bulbous endings. The least common are mushroom-shaped and have thick stalks ending in large bulbs. Other spines are short and stubby without well-defined stalks.

Several suggestions have been made about the functional significance and behavior of dendritic spines; some of which have important implications in synaptic plasticity. These include the following. (*a*) Chang (1952) first pointed out that the high resistance of a thin spine stem would attenuate the effect of synaptic input delivered to the spine head upon the postsynaptic neuron. (*b*) Rall (1970) stated as follows. "My own preference is to point out that spine stem resistance could be an important variable which might be used physiologically to change the relative weights of synaptic inputs from different afferent sources; this could provide a basic mechanism for learning in the nervous system. " (*c*) Tsukahara and Oda (1981) pointed out that the shortening of dendritic spines of red nucleus neurons can be considered one of the possible mechanisms for shortening the time-to-peak of cortico-rubral excitatory postsynaptic potentials, which is seen after establishment of classical conditioning. (*d*) Crick (1982) hypothesized that there are contractile proteins associated with each spine that enable the spine to change its shape rapidly during neuronal activity. The twitch of the spine would produce a very rapid change in the effectiveness of the synapse on the spine. This might provide a possible mechanism for a very short term memory.

Morphological changes of spines take place under various environmental conditions. For example, it is well known that the number of spines of pyramidal cells in the visual cortex changes when animals are kept in darkness during early developmental stages (Valverde, 1967). Moreover, two groups of authors (Fifkova and van Harreveld, 1977; Lee et al., 1980) have presented experimental evidence that spines in the hippocampus can change shape as a result of the kind of massive stimulation that produces postactivation potentiation. Katsumaru et al. (1982) demonstrated the presence of actin in dendritic spines of red nucleus neurons. This might provide a molecular basis for morphological changes of dendritic spines.

Rall (1974, 1978) and Jack et al. (1975) have already done theoretical studies of spines to assess the quantitative significance of the above suggestions. Unfortunately their published results were confined to only steady state condi-

tions. Jack et al. (1975) treated the parent dendrite to which the spine stem is attached as an infinite cable. Wilson (1982) has presented a report on the transient behavior of the spine in the same simplified dendritic geometry. If the parent dendrite is very short and its peripheral end is sealed, their treatment is not sufficient. To evaluate changes of postsynaptic potentials associated with morphological changes of dendritic spines, it is desirable to study transient behavior of spines in neurons with arbitrary dendritic geometries. Although we (Kawato and Tsukahara, 1983) investigated transient electrical properties of spines in our previous paper, we treated a spine as a cylinder and neglected the effect of end bulbs. Because almost all spines have their end bulbs, in this paper we incorporate the effect of end bulbs into our model as one of the boundary conditions.

We reduced postsynaptic potential transform produced by a synapse on a dendritic spine into a product of two transfer functions and the synaptic input current transform, according to Butz and Cowan's theorem (1974). The first transfer function is the Laplace transform of an impulse response function of the neuron and is determined to be independent of the spine. The second transfer function is concerned mainly with the spine and represents the straightforward attenuation effect of the spine. The synaptic input current might be reduced if the extra resistance of the spine stem chokes back the ionic current flow during synaptic activation. We quantitatively evaluate changes of postsynaptic potential associated with morphological changes of the spine by examining both the second transfer function and the synaptic input current.

POSTSYNAPTIC POTENTIAL CAUSED BY A SYNAPSE ON A DENDRITIC SPINE

Our model starts with the well-established cable equation representation (Rall, 1959) of electrotonic potentials. The major assumptions are the following (*a*) All dendritic branches are cylinders of uniform passive nerve membrane. (*b*) The extracellular space is an isopotential. (*c*) Each unit membrane is connected to its neighbors by core resistance, so that each cylinder is regarded as a one-dimensional cable of finite length. (*d*) At all branch points membrane potential is assumed to be continuous, and core current is conserved. With the above assumptions one can derive the cable equation for the membrane potential $v(x,t)$ and the equation for the core current $i(x,t)$

$$\lambda^2[\partial^2 v(x,t)/\partial x^2] - \tau \partial v(x,t)/\partial t - v(x,t) = 0, \quad (1)$$

$$i(x,t) = -(1/r_i)\,[\partial v(x,t)/\partial x], \quad (2)$$

where x is the position along some branch of the dendritic tree, t is time. $\tau = r_m c_m = R_m C_m$ and $\lambda = \sqrt{r_m/r_i} = \sqrt{R_m a/2R_i}$ are called the membrane time constant and the cylinder space constant of the branch, respectively. R_i, R_m, C_m, a, r_i, r_m, c_m are, respectively, the intracellular resistivity, the membrane resistance, the membrane capacitance, the cylinder radius, the intracellular resistance to axial flow of current along cylinder, the membrane resistance per unit length cylinder, and the membrane capacitance per unit length cylinder. These parameters may be different for different branches.

Let $V(x,p)$ and $I(x,p)$ be the Laplace transforms of $v(x,t)$ and $i(x,t)$.

$$V(x,p) = \int_0^\infty v(x,t)e^{-pt}dt, \quad (3)$$

$$I(x,p) = \int_0^\infty i(x,t)e^{-pt}dt, \quad (4)$$

The general solution is easily written as

$$V(x,p) = C(p)\cosh \gamma x + D(p)\sinh \gamma x, \quad (5)$$

$$I(x,p) = -(1/Z)\,[C(p)\sinh \gamma x + D(p)\cosh \gamma x], \quad (6)$$

where

$$\gamma = q/\lambda, \quad (7)$$

$$q = \sqrt{\tau p + 1}, \quad (8)$$

$$Z = r_i/\gamma. \quad (9)$$

Z is known as the characteristic impedance of the cable.

To study the postsynaptic potential caused by a synapse on a dendritic spine, we consider a spine located at a point M levels of branching in the neuron with arbitrary dendritic geometry (Fig. 1). There is no loss of generality in considering this special case. All dendritic branches are treated as cylinders. It is important to consider boundary conditions that approximate the effects of end bulbs of dendritic spines. The simplest procedure is to represent them as a lumped impedance $B_h = 1/S_h(C_{mh}p + 1/R_{mh}) = (R_{mh}/S_h)/(\tau_h p + 1) = R_h/(\tau_h p + 1)$ at the peripheral boundary of the spine stalk. S_h, R_{mh}, C_{mh}, $\tau_h = R_{mh}C_{mh}$, R_h are, respectively, surface area, the membrane resistance, the membrane capacitance, the membrane time constant, and the total membrane resistance of the spine head. Thus, in our model, the spine is represented by a cylinder of length l_s with a terminal impedance B_h (see Fig. 1). The postsynaptic terminal on the spine is located at the head of

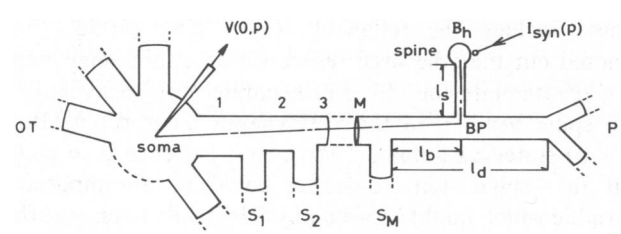

FIGURE 1 Dendritic configuration of the neuron with the dendritic spine of length l_s. The effect of the spine head is represented by the terminal impedance B_h. The chain line indicates the direct path from the soma ($x = 0$) at which the postsynaptic potential is recorded to the location of the synaptic current source at the spine head. See text for detail.

the spine. The spine stalk becomes continuous with the main dendritic trunk of length l_d at a branching point l_b ($l_b \leqq l_d$) along the cylinder corresponding to the parent dendrite. This branching point is called BP. The dendritic tree that is attached to the distal end of the parent dendrite is simply called P. There are M branches proximal to the opposite end of the parent dendrite along the direct path from the spine to the soma. These branches are represented by the first, second, ... Mth cylinder. M dendritic subtrees, which are continuous with the direct path from the spine to the soma, are designated as the first subtree S_1, second subtree S_2, ... Mth subtree S_M. Apart from the dendritic tree containing the spine in question, several dendritic trees may radiate from the soma. These are collectively designated OT. To incorporate a lumped impedance, which represents the effect of the soma, one of the OT is assumed to be very short and to have the boundary impedance $B_{soma} = 1/(C_{soma}p + G_{soma})$. The total dendritic tree of the neuron in Fig. 1 may have many dendritic spines other than the spine in question.

Z_k (k = 1, 2, ..., M) represents the characteristic impedance (see Eq. 9) of the kth branch. Z_{M+k} (k = 1, 2, ..., M) represents the characteristic impedance of the dendritic branch, which is continuous with the direct path from the spine to the soma, of the kth subtree S_k. a_s, γ_s, and Z_s, respectively, denote the spine radius, γ, of the spine (see Eq. 7), and the characteristic impedance of the spine. Similarly a_d, γ_d, and Z_d represent those quantities of the parent dendrite.

With this notation Butz and Cowan's theorem (1974) facilitates calculations of the membrane potential transform for any electrical activity in the neuron of Fig. 1 (see Appendix A for Butz and Cowan's theorem). In particular, the postsynaptic membrane potential transform, $PSP(p)$, at the soma caused by the synapse on the spine is derived and given by Eq. B1 in Appendix B. Although Eq. B1 is simple in its form, it is still far from useful for understanding electrical properties of dendritic spines. Horwitz (1981) recently developed the analytical method with which one can calculate the Laplace inverse of Butz and Cowan's solution. However, since he assumed a special symmetry in a simple dendritic tree, we cannot use his result.

To investigate the change in the postsynaptic potential associated with a morphological change of the spine as a potential mechanism underlying synaptic plasticity, we resolve the postsynaptic potential transform as follows.

$$PSP(p) = K(p) \cdot H(p) \cdot I_{syn}(p) = K(p) \cdot I_{eff}(p). \quad (10)$$

The derivation is given in Appendix B. Hereafter we use several symbols that are defined in Appendix B and C. However, when a new symbol first appears in the text, we will always explain its meaning and state where it is defined in the Appendix. $K(p)$, which is defined by Eq. B2, is the transfer function between the branching point, BP, and the soma. As seen from Eq. B2, $K(p)$ is Laplace transform of voltage transient, $k(t)$, at the soma of the neuron without the spine, which is otherwise the same as the original neuron, in response to a pulse current in the form of Dirac delta function injected at the point that corresponds to BP where the spine was attached in the original neuron. $I_{syn}(p)$ denotes the Laplace transform of the synaptic current input, $i_{syn}(t)$. $I_{eff}(p)$ is the Laplace transform of the effective electric current, $i_{eff}(t)$, which flows into the parent dendrite from the spine stem via the BP (see Fig. 2). $H(p)$ is defined by Eq. B3 and can be interpreted as the transfer function that represents the straightforward attenuation effect of the spine transforming the synaptic current into the effective current.

The relation $I_{eff}(p) = H(p) \cdot I_{syn}(p)$ in Eq. 10 can be derived without the Butz and Cowan graphical notation as follows. We assume that the intracellular resistivity, R_i, of the spine and the parent dendrite are the same. We further assume that the membrane resistance, R_m, and the membrane capacitance, C_m, are common to the parent dendrite, the spine stalk, and the spine head. Then, the membrane time constant, τ, is also common to these structures. In this case the following equations hold true.

$$Z_d/Z_s = (a_s/a_d)^{3/2}, \quad (11)$$

$$Z_s/B_h = q/\rho_{sh}, \quad (12)$$

where ρ_{sh} is stalk-head conductance ratio and is defined as

$$\rho_{sh} = B_h(0)/Z_s(0) = R_h/r_{is}\lambda_s = \pi \sqrt{2R_m/R_i}\, a_s^{3/2}/S_h. \quad (13)$$

ρ_{sh} is much larger than one for usual configurations of spines, but it might become close to one for a spine with a very thin stalk and a large end bulb.

The current transform across the spine-head membrane, $I_h(p)$, can be expressed

$$I_h(p) = V_h(p)/B_h(p) = (q/\rho_{sh}Z_s)V_h(p) = (q/\rho_{sh}Z_s)V_s(l_s, p), \quad (14)$$

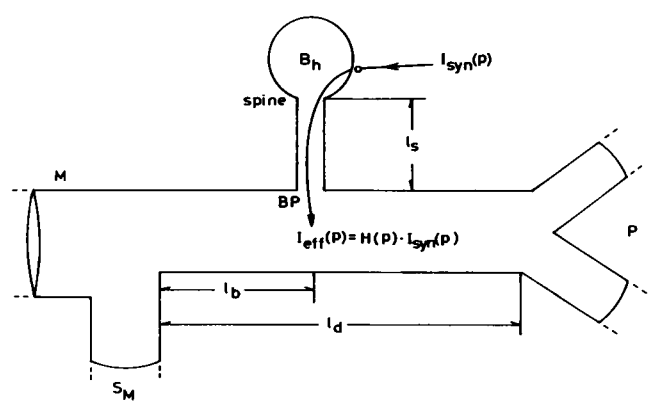

FIGURE 2 Magnification of the neuron in Fig. 1 around the spine. $I_{eff}(p) = H(p) \cdot I_{syn}(p)$ denotes the effective current transform which reaches the parent dendrite.

where $V_h(p)$ and $V_s(x, p)$ are the voltage transforms of the spine head and the spine stem at point x. The boundary condition at the spine head can be expressed

$$I_{syn}(p) = I_h(p) - I_s(l_s, p), \tag{15}$$

where $I_s(x, p)$ is the axial current transform of the spine stem at point x. The other boundary condition for the spine stem at the BP is

$$V_s(0, p) = I_{eff}(p) \cdot Z_{in}(p) = I_s(0, p) \cdot Z_{in}(p), \tag{16}$$

where $Z_{in}(p)$ represents the input impedance function of the parent dendrite at the point where the spine is attached. The use of these boundary conditions with Eqs. 5 and 6 leads to

$$\begin{aligned} 1/H(p) &\equiv I_{syn}(p)/I_{eff}(p) \\ &= \cosh \gamma_s l_s + (q/\rho_{sh}) \sinh \gamma_s l_s \\ &\quad + [Z_{in}(p)/Z_s(p)] \\ &\quad \cdot [\sinh \gamma_s l_s + (q/\rho_{sh}) \cosh \gamma_s l_s]. \end{aligned} \tag{17}$$

Eq. 17 is equivalent to the definition of $H(p)$, Eq. B3. However, the explicit expression of $H(p)$ is essential to evaluate the straightforward attenuation effect of the spine quantitatively. Eq. B3 can be rewritten on the above assumptions into a form for which comparison with Eq. 17 is easy

$$\begin{aligned} 1/H(p) &= \cosh \gamma_s l_s + (q/\rho_{sh}) \sinh \gamma_s l_s \\ &\quad + (a_s/a_d)^{3/2} F(p) \\ &\quad \cdot [\sinh \gamma_s l_s + (q/\rho_{sh}) \cosh \gamma_s l_s]. \end{aligned} \tag{18}$$

Derivation of Eq. 18 and explicit expression of $F(p)$ are given in Appendix C. Eq. 18 can also be obtained by substituting the explicit Butz and Cowan's expression of $Z_{in}(p)$ into Eq. 17.

Eq. 10 can be represented in the time domain as follows

$$\begin{aligned} psp(t) &= \int_0^t k(u) \left[\int_0^{t-u} h(w) i_{syn}(t - u - w) \mathrm{d}w \right] \mathrm{d}u \\ &= \int_0^t k(u) i_{eff}(t - u) \mathrm{d}u, \end{aligned} \tag{19}$$

where

$$i_{eff}(t) = \int_0^t i_{syn}(u) h(t - u) \mathrm{d}u. \tag{20}$$

$h(t)$ is the inverse Laplace transform of $H(p)$. $psp(t)$ is the postsynaptic potential caused by the synapse on the spine, and hence is the inverse Laplace transform of $PSP(p)$.

Eq. 19 can be regarded as the superposition principle of a linear system. Then $k(t)$ is regarded as an impulse response function of the neuron without the spine, and $i_{eff}(t)$ as an input to the neuron without the spine. If the synapse is located directly on the parent dendrite, then the postsynaptic potential, $psp^*(t)$, of the neuron without the spine is

$$psp^*(t) = \int_0^t k(u) i_{syn}(t - u) \mathrm{d}u. \tag{21}$$

Hence, the $psp(t)$ of the neuron with the spine is represented as follows

$$psp(t) = \int_0^t psp^*(u) h(t - u) \mathrm{d}u. \tag{22}$$

While $h(t)$ was interpreted from Eq. 20 as the filter that represents the straightforward attenuation effect of the spine transforming the synaptic current, $i_{syn}(t)$, into the effective current, $i_{eff}(t)$, it can also be regarded from Eq. 22 as the straightforward attenuation factor of the postsynaptic potential due to the spine. Because $K(p)$ or $k(t)$ depends only on the dendritic tree other than the spine, it is not affected by a conformation change of the spine. On the other hand, $h(t)$ and $i_{syn}(t)$ are determined mainly by electrical and morphological characteristics of the spine. Although $h(t)$ represents the straightforward attenuation effect of the spine, $i_{syn}(t)$ might also change because the synaptic activation involves a transient change of conductance at the synapse. The extra resistance of the spine neck might choke back the resultant flow of ions during synaptic activation. To quantitatively assess the suggestions made in the Introduction, we evaluate the straightforward attenuation effect in the next section. Then the second attenuation effect will be examined. If one notices the perfect symmetry between the stimulus site and the recording site in Butz and Cowan's theorem, it is quite easy to prove the following proposition in a way similar to the derivation of Eq. 19.

Proposition

The transient membrane potential $v_s(l_s, t)$ at the spine head, in response to current input applied anywhere on the dendritic tree except on the spine, is expressed as the following convolution integral

$$v_s(l_s, t) = \int_0^t v_d^*(l_b, u) h(t - u) \mathrm{d}u, \tag{23}$$

where $v_d^*(l_b, t)$ is the transient voltage at the point that corresponds to BP in response to the same input current applied at the same point as in the original case, of the neuron without the spine, which is otherwise the same as that of Fig. 1.

The proposition provides us with the mathematical tool with which we can quantitatively assess the suggestion that the dendritic spine provides a postsynaptic region that is effectively isolated from other synapses in the neuron.

QUANTITATIVE ASSESSMENT OF THE STRAIGHTFORWARD ATTENUATION EFFECT OF THE DENDRITIC SPINE

In this section, we quantitatively evalute $h(t)$ using morphological parameters describing the size and shape of

dendritic spines, which are known from histology. In Appendix D we prove that $F(p)$ of Eq. 18, which is defined by Eq. C2, is at most on the order of 1 ($F[p] \sim 0[1]$). We now make a major assumption.

Assumption

The diameter of the spine, $2a_s$, is very small compared with the diameter, $2a_d$, of the parent dendrite to which the spine stem is attached. To state this more explicitly, we assume

$$(a_s/a_d)^{3/2} \ll 1. \tag{24}$$

Jack et al. (1975) take, as an example, a parent dendrite diameter of 5 μm and a spine stalk diameter of 0.2 μm. This leads to $(a_s/a_d)^{3/2} = 0.008$, which is sufficient for our purpose. It has been reported, for several neuron types, that dendritic spines with long and thin spine stems occur more frequently on the more distal dendritic branches of small diameter, while stubby dendritic spines occur more frequently on dendritic trunks and the more proximal dendritic branches of larger diameter. This observation also supports our assumption. We would like, in this section, to examine the consequence of this assumption about morphological features of dendritic spines.

From the above assumption and the fact that $F(p) \sim O(1)$, we can neglect the third term of Eq. 18

$$H(p) \simeq G(p) = 1/[\cosh \gamma_s l_s + (q/\rho_{sh}) \sinh \gamma_s l_s]. \tag{25}$$

We can get the inverse Laplace transform $g(t)$ of $G(p)$

$$\begin{aligned} g(t) = {} & \sqrt{2/\pi}/(\tau T) \cdot e^{(\rho_{sh}^2/2-1)T} \\ & \cdot \sum_{n=0}^{\infty} e^{(n+1/2)\rho_{sh} L_s} \cdot e^{-(n+1/2)^2 L_s^2/(2T)} \\ & \cdot \sum_{r=0}^{n} [(-n)_r/r!] 2^{3r/2} \cdot \rho_{sh}^{r+1} \\ & \cdot T^{r/2} \cdot \{(r+1)\sqrt{2T}\, D_{-r-2} \\ & \cdot [\rho_{sh}\sqrt{2T} + (2n+1) L_s/\sqrt{2T}] \\ & + (2n+1) L_s D_{-r-1} \\ & \cdot [\rho_{sh}\sqrt{2T} + (2n+1) L_s/\sqrt{2T}]\}, \end{aligned} \tag{26}$$

where $T = t/\tau$ and

$$L_s = l_s/\lambda_s = \sqrt{2R_i/R_m}\, l_s a_s^{-1/2}. \tag{27}$$

L_s is the electrotonic length of the spine stalk and $D_n(x)$ is the parabolic cylinder function. The derivation of Eq. 26 is given in Appendix E.

Let Q_{eff} denote the total electric charge that flows into the parent dendrite via the bifuraction point BP

$$\begin{aligned} Q_{eff} \simeq Q_{syn} \int_0^{\infty} g(t)\mathrm{d}t = Q_{syn} G(0) \\ = Q_{syn}\, \rho_{sh}/(\sinh L_s + \rho_{sh} \cosh L_s). \end{aligned} \tag{28}$$

Here Q_{syn} denotes the total electrical charge injected at the

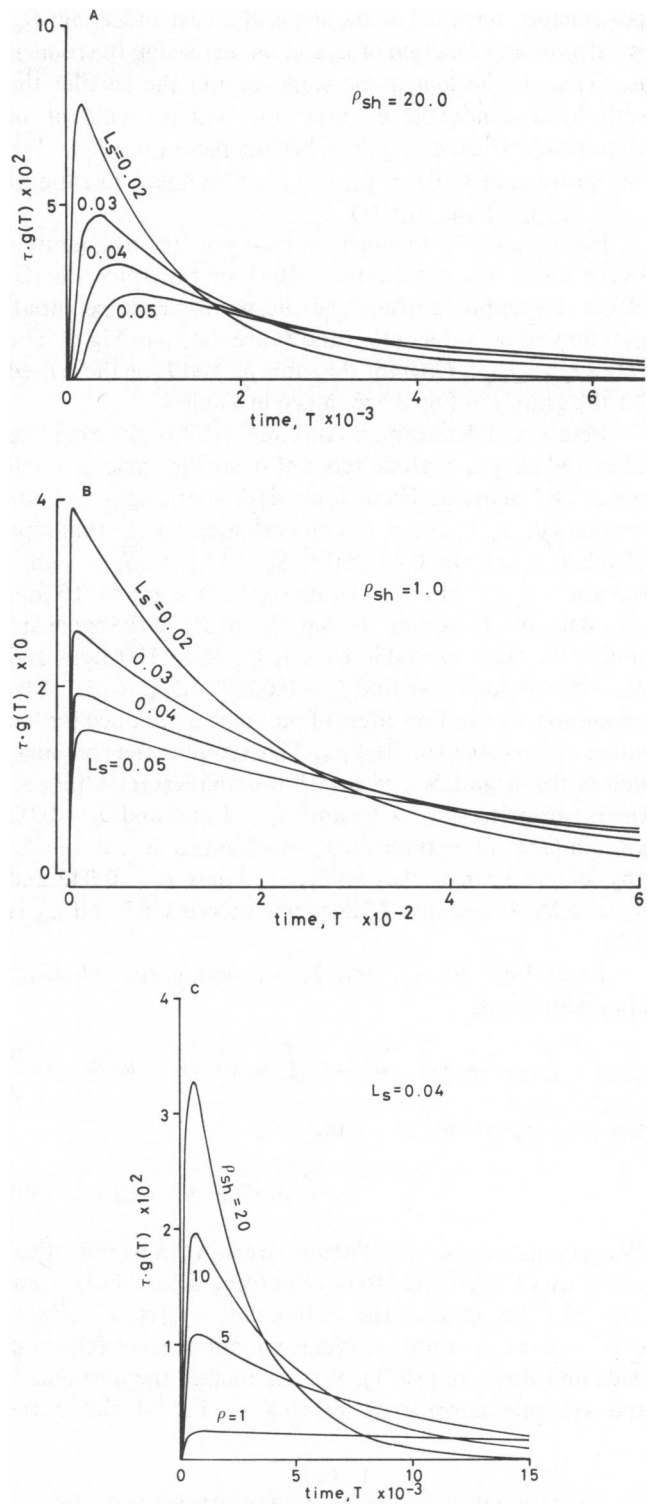

FIGURE 3 $\tau g(t)$ of Eq. 26 is shown as a function of T. Numerals attached to curves in the figure indicate values of the electrotonic length of the spine, L_s, or stalk-head conductance ratio, ρ_{sh}. $g(t)$ determines the straightforward attenuation effect of the spine. Note that $g(t)$ has dimension ms^{-1}, so $\tau g(t)$ is dimensionless. Calculation was done on a computer summing up at least the first 10 terms in Eq. 26 and up to higher terms so that an error is <0.0001. *A* shows $\tau g(t)$ when $\rho_{sh} = 20.0$ and L_s has values of 0.02, 0.03, 0.04, and 0.05. *B* shows it when $\rho_{sh} = 1.0$. *C* shows $\tau g(t)$ when $L_s = 0.04$ and ρ_{sh} has values of 1, 5, 10, and 20.

postsynaptic terminal on the spine. It is easy to see that Q_{eff} is a decreasing function of L_s and an increasing function of ρ_{sh}. That is, the longer the spine is, and the smaller the stalk-head conductance ratio, the smaller amount of injected electrical charge reaches the parent dendrite. We can prove that $G(0) \cong Q_{eff}/Q_{syn}$ is also equal to ratio of areas of $psp(t)$ and $psp^*(t)$.

Eqs. 26 and 28 together make it possible to quantitatively assess the attenuation effect of the spine on the effective synaptic current and the postsynaptic potential. $g(t)$ for various values of ρ_{sh} and L_s are shown in Fig. 3. The ratios $Q_{eff}/Q_{syn} \cong G(0)$ for the same ρ_{sh} and L_s as those used for the graphs in Fig. 3 are shown in Table I.

Peters and Kaiserman-Abramof (1970) reported the sizes and shapes of three types of dendritic spine of small pyramidal neurons. From their data the ranges and the averages of S_h, l_s, and a_s can be evaluated for the thin type of spines. They are: $0.13\ \mu m^2 < S_h < 13\ \mu m^2$, $\bar{S}_h = 1\ \mu m^2$, $0.3\ \mu m < l_s < 3\ \mu m$, $\bar{l}_s = 1\ \mu m$, $0.02\ \mu m < a_s < 0.15\ \mu m$, $\bar{a}_s = 0.05\ \mu m$. If we assume that R_i and R_m of the spine are similar to other excitable cells (e.g., $R_i = 100\ \Omega cm$ and $R_m = 5{,}000\ \Omega cm^2$), we find $\bar{L}_s = 0.0089$ and $\bar{\rho}_{sh} = 35.1$. The maximum attenuation effect of the spine is obtained for the largest L_s and the smallest ρ_{sh}. This requires the combination of the largest S_h and l_s with the smallest a_s. Although these parameters, $S_h = 13\ \mu m^2$, $l_s = 3\ \mu m$, and $a_s = 0.02\ \mu m$, induce an extraordinary configuration out of the physiological range, they still lead to only $L_s = 0.042$ and $\rho_{sh} = 0.68$. Generally, L_s does not exceed 0.05 and ρ_{sh} is >1.0.

From Eqs. 20, 22, and 25 we obtain the following approximations.

$$i_{eff}(t) = \int_0^t i_{syn}(u)h(t-u)\,du \simeq \int_0^t i_{syn}(u)g(t-u)\,du, \quad (29)$$

$$psp(t) = \int_0^t psp^*(u)h(t-u)\,du \simeq \int_0^t psp^*(u)g(t-u)\,du. \quad (30)$$

We present some simple illustrative examples by numerical calculations. First the effective current is calculated from Eq. 29. We choose the α-function, $i_{syn}(t) = \alpha^2(t/\tau)\exp(-\alpha t/\tau)$, as a time varying synaptic current following Jack and Redman (1971). We can modify the duration of the synaptic current by varying α. Fig. 4 shows the

TABLE I
RATIOS OF Q_{eff} AND Q_{syn} FOR VARIOUS VALUES OF L_s and ρ_{sh}: $G(0) \simeq Q_{eff}/Q_{syn}$

ρ_{sh}	L_s			
	0.02	0.03	0.04	0.05
1.0	0.980	0.970	0.961	0.951
5.0	0.996	0.994	0.991	0.989
10.0	0.998	0.996	0.995	0.994
20.0	0.999	0.998	0.997	0.996

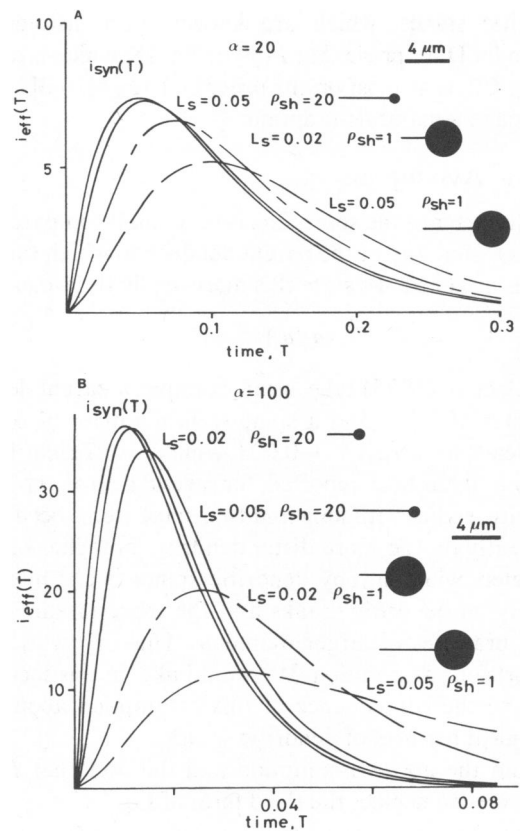

FIGURE 4 The effective electrical current that flows into the parent dendrite for various values of L_s and ρ_{sh}. The α-function is chosen as the synaptic current and α is 20 in *A* and 100 in *B*. The bar indicates 4 μm for insets showing shapes of spines. See text for details.

effective current as a function of time. The curve on the far left represents the synaptic current. The effective current was calculated for the following geometrical parameter values (L_s, ρ_{sh}) = (0.02, 20), (0.05, 20), (0.02, 1), and (0.05, 1). The insets in Fig. 4 show examples of the corresponding shapes of spines for $R_i = 100\ \Omega cm$, $R_m = 5{,}000\ \Omega cm^2$, and $a_s = 0.05\ \mu m$. As these insets clearly indicate, the values (0.02, 1) and (0.05, 1) are apparently out of the physiological range. The value (0.05, 20) might be on the border of the physiological range. The value (0.02, 20) is inside the physiological range but it produces the stronger effect than the average value (0.0089, 35.1). In Fig. 4 *a* relatively long duration of the synaptic current ($\alpha = 20$) is chosen. In this case the effective current for (0.02, 20) is almost identical to the synaptic current and hence cannot be drawn. Even the value on the border of the physiological range (0.05, 20) produces only a small attenuation effect on the effective current. The effective currents for values outside the physiological range are drawn by a chain line for (0.02, 1) and a broken line (0.05, 1). On the other hand, for short duration of the synaptic current (see Fig. 4 *b* for $\alpha = 100$), even the value (0.02, 20) inside the physiological range, slightly attenuates the effective current. For the value (0.05, 20) the attenuation effect is not negligible.

Second, we numerically calculated the postsynaptic potential from Eq. 30 in a simple model shown in Fig. 5. In the model, whole dendritic geometry is replaced by an equivalent cylinder of electronic length 1.1. The same synaptic current of α-function is injected at the spine head, which is located at the electrotonic distance of 0.6 from the soma. Although we deal with only one dendritic spine on one dendrite in this model, it is essentially equivalent to the case where every dendrite has a spine at the same electrotonic distance from the soma. For, if one spine causes, for example, 1% change in the postsynaptic potential shape, any number of spines cause exactly the same 1% change because of linear summation of postsynaptic potentials. Figs. 6 *a* and *b* show the postsynaptic potential for $\alpha = 20$ and $\alpha = 100$. The solid curve represents the postsynaptic potential $psp^*(T)$, which is caused by the synapse located directly on the parent dendrite. The postsynaptic potentials for values (0.02, 20) and 0.05, 20) are almost identical to $psp^*(T)$ and hence cannot be drawn for both cases of $\alpha = 20$ and $\alpha = 100$. The change of peak amplitude is <0.5% for these spines. The chain line and the broken line indicate the postsynaptic potentials for extraordinary shapes of spines outside the physiological range. Hence, the straightforward attenuation effect on the postsynaptic potential is negligible irrespective of the duration of the synaptic current.

We can draw general conclusions from these examples. From the nature of the convolution integrals in Eqs. 29 and 30, clearly $g(t)$, which is much shorter than the duration of $i_{syn}(t)$ or $psp^*(t)$ and whose area is almost equal to 1, will give a small contribution. As shown in Table I, $\int_0^\infty g(t)dt = G(0) \cong Q_{eff}/Q_{syn}$ is almost equal to 1 for physiological ranges of parameters. On one hand, the duration of $g(t)$ is shorter than 1/100 of the membrane time constant for physiological ranges of geometrical parameters as seen from Fig. 3. (Note that scales of abscissa in Fig. 3 are either 1/1,000 or 1/100 of the membrane time constant.) On the other hand, the duration of postsynaptic potentials is usually longer than 1/10 of the membrane time constant (see Tsukahara and Kosaka [1968], for example). Hence, $g(t)$ is very close to the Dirac delta function in the above sense and $psp(t)$ is almost identical to $psp^*(t)$. Thus, the postsynaptic potential due to the synapse on the spine is

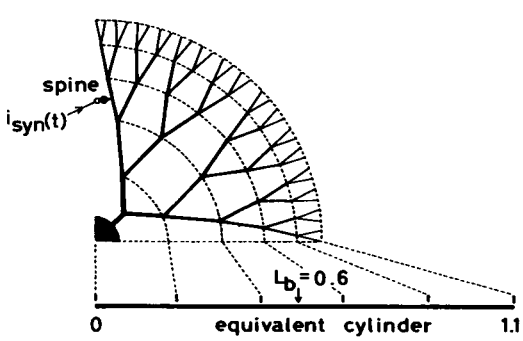

FIGURE 5 A simple equivalent cylinder model with the dendritic spine.

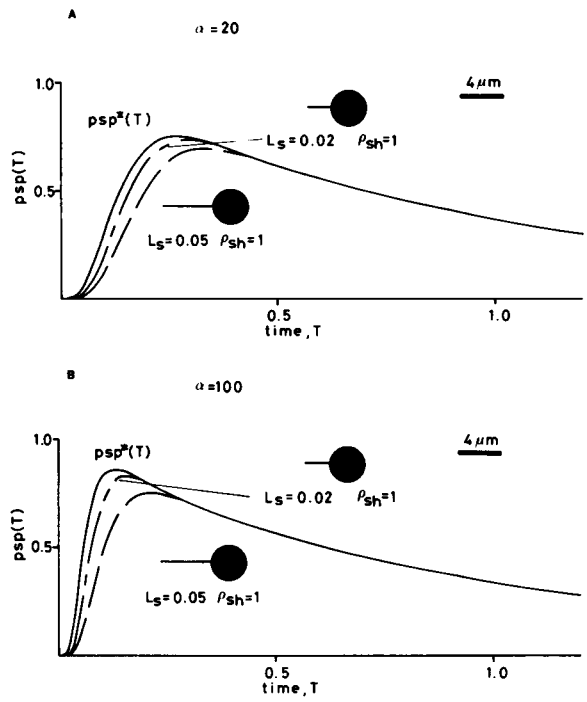

FIGURE 6 The postsynaptic potential in the simple model of Fig. 5 for various values of L_s and ρ_{sh}. α is 20 in *A* and 100 in *B*. See text for detail.

almost equal to the postsynaptic potential caused by the synapse on the parent dendrite if the synaptic input current is the same for both cases. Therefore, a morphological change of the spine, if it were to take place, would lead to only negligible changes in the postsynaptic potential, when the synaptic current remains unaltered, which is the case for a large synaptic resistance as compared with the spine stem resistance.

Experimental evaluation of synaptic activation time, $i_{syn}(t)$, is more difficult than that of the postsynaptic potential. However, in red nucleus neurons the duration of $i_{syn}(t)$ is evaluated to be longer than 1/10 of the membrane time constant (Tsukahara et al., 1975). Consequently, $i_{eff}(t)$ is almost identical to $i_{syn}(t)$. However, if synaptic activation time is very short (say 1/100 or 1/1,000 of the membrane time constant), the shape of $i_{eff}(t)$ is different from that of $i_{syn}(t)$. Note that the change of the postsynaptic potential is negligible even in this case. Consequently, we can still generally state that the straightforward attenuation effect of spines is negligible because the effective current has much less relevance to synaptic plasticity than the postsynaptic potential.

Similarly to the above discussion, the proposition in the preceding section reveals that the isolation effect of the spine on the synapse from the electrical activity of a neighboring synapse is negligible unless it is very rapid (whose duration is shorter than 1/100 or 1/1,000 of the membrane time constant). This point has been noted previously by Jack et al. (1975). It is also implicit in Rall and Rinzel (1973) and Rinzel and Rall (1974).

EVALUATION OF THE ATTENUATION EFFECT OF THE DENDRITIC SPINE ON THE SYNAPTIC CURRENT

The synaptic input current, $i_{syn}(t)$, might be reduced if the extra resistance of the spine stem chokes back the ionic current flow during synaptic activation. In this section, we present conditions for the change of the synaptic current associated with a morphological change of the spine. The synaptic input current satisfies the equation

$$i_{syn}(t) = g_{syn}(t) \cdot [v_{rev} - v_s(l_s, t)], \tag{31}$$

where v_{rev} is the reversal potential of the synapse, and $v_s(l_s, t)$ is the membrane potential at the spine head. Let us assume, for simplicity, that the synaptic conductance, $g_{syn}(t)$, changes in the form of a rectangular pulse

$$g_{syn}(t) = \begin{cases} 0 \; t < 0, w < t \\ 1/R_{syn} \; 0 < t < w. \end{cases} \tag{32}$$

Then the synaptic input current, $i_{syn}(t)$, is given as follows

$$i_{syn}(t) = \begin{cases} 0 \; t < 0, w < t \\ j(t) \; 0 < t < w, \end{cases} \tag{33}$$

where $j(t)$ is an inverse Laplace transform of the following function

$$J(p) = (v_{rev}/p) \cdot 1 \Bigg/ \left(R_{syn} + 1 \Bigg/ \left\{ \frac{1}{B_h} + \frac{Z_s + Z_d F(p) \tanh \gamma_s l_s}{Z_s [Z_s \tanh \gamma_s l_s + Z_d F(p)]} \right\} \right). \tag{34}$$

We assume that $(a_s/a_d)^{3/2} \ll 1$ and that $B_h \gg Z_s \tanh \gamma_s l_s + Z_d F(p)$, which is quite reasonable because $L_s \ll 1$. Then, $J(p)$ can be approximated by the simpler expression

$$\begin{aligned} J(p) &\simeq v_{rev}/p \, [R_{syn} + Z_s \tanh \gamma_s l_s + Z_d F(p)] \\ &= v_{rev}/p \{R_{syn} + Z_s [\tanh \gamma_s l_s + (a_s/a_d)^{3/2} F(p)]\}. \end{aligned} \tag{35}$$

Here the second term in the denominator is the input impedance of the spine stalk. The third term in the denominator is the input impedance of the dendritic tree at BP. When the spine changes its shape, only the second term of the denominator changes in the right-hand side of Eq. 35. Hence, conditions for the change of $i_{syn}(t)$, which is associated with the morphological change of the spine, are the following. (*a*) The input impedance of the spine stalk must be comparable with the input impedance of the dendritic tree at BP. (*b*) The input impedance of the spine stalk must be comparable with the synaptic resistance. We illustrate these conditions in two extreme cases. The first case is the long duration of conductance changes. In this case the conditions become

$$Z_s(0) \tanh L_s \gtrsim Z_d(0) \cdot F(0),$$

$$\text{i.e., } L_s (a_d/a_s)^{3/2} \gtrsim F(0) \sim O(1)), \tag{36}$$

$$Z_s(0) \tanh L_s \gtrsim R_{syn}. \tag{37}$$

The first condition has been pointed out by Rall (1974, 1978), although his discussion does not contain a geometric view point. Because L_s is much smaller than one, this condition requires that $(a_s/a_d)^{3/2} \ll 1$. Let us examine the second condition. If we adopt the value $R_i = 100$ Ωcm, $Z_s(0) \tanh L_s \cong (R_i l_s)/(\pi a_s^2)$ has a range 4.3×10^6 Ω ~ 2.4×10^9 Ω given the following ranges of parameters: 0.3 μm < l_s < 3 μm, 0.02 μm < a_s < 0.15 μm. Rall (1978) implicitly assumed that the spine stem resistance, $Z_s(0) \cdot \tanh L_s$, is either nearly equal to R_{syn} or else ten times as large. On the other hand, if we take a value $R_{syn} = 10^9$ Ω as Jack et al. (1975) adopted as an illustrative value, the synaptic input current does not change effectively for almost all dendritic spines. The actual size of the synaptic resistance change on a spine is still an open question. Barrett and Crill (1974) estimated the synaptic resistance, which produces unitary excitatory postsynaptic potential (EPSP) in motoneurons, as being on the order of 10^8 Ω. Our preliminary estimation of the synaptic resistance for unitary EPSP in red nucleus neurons also suggests an order of 10^8 Ω. In consideration of the possibility that the unitary postsynaptic potentials in the central nervous system might be produced by activation of many synaptic terminals, single synaptic resistance on a spine may be $>10^9$ Ω. In this case, the dendritic spine has no electrical function in the brain. Anyway, whether the synaptic resistance is larger than the spine stem resistance or not is the important, unresolved aspect of the overall problem.

We consider the second extreme case of very rapid conductance changes. Let $\omega (\gg 1)$ denote the main frequency of the conductance change. Then we can replace p by $j\omega$. If R and Y denote real and imaginary parts of $\sqrt{1 + j\tau\omega}$, then both R and Y are large for large ω. Because of the hyperbolic identity, the following equation holds true

$$\begin{aligned} \tanh(\gamma_s l_s) &= \tanh(L_s R + jL_s Y) \\ &= [\sinh(2L_s R) + j \sin(2L_s Y)]/ \\ &\quad [\cos h(2L_s R) + \cos(2L_s Y)] \\ &\simeq \tanh(2L_s R) \simeq 1. \end{aligned} \tag{38}$$

Consequently, the first condition is always satisfied. The second condition becomes

$$\begin{aligned} &|(r_i \lambda \sqrt{1 + j\tau\omega}) \tanh(\sqrt{1 + j\tau\omega} L_s)| \\ &\quad = |[r_i \lambda/(R + jY)] \tanh(L_s R + jL_s Y)| \gtrsim R_{syn}. \end{aligned} \tag{39}$$

This condition is severer than that in Eq. 37 because both R and Y are large. Physiologically, this corresponds to the fact that the spine stalk does not provide an effective impedance for very brief current.

From these results for two extreme cases, we can conclude that the synaptic current does not change effectively associated with change of the spine for any synaptic

conductance change if the synaptic resistance is very large compared with the spine stalk resistance.

DISCUSSION

Our conclusion that dendritic spines have no significant electrical functions when the synaptic resistance is large as compared with the spine stem resistance, depends on several assumptions. We will discuss them in order.

First, we evaluated L_s and ρ_{sh} on the assumption that the intracellular resistivity, R_i, and the membrane resistance, R_m, of spines are similar to other excitable cells. Jones and Powell (1969) reported that the cytoplasm of a spine looks a little different in the electron microscope from that in the adjacent dendritic shaft, the former being somewhat denser and also flocculent in appearance. Peters and Kaiserman-Abramof (1970) reported that the spine apparatus is present in most spines, particularly in large ones. These observations might imply a high intracellular resistivity. As we have shown in Eqs. 13 and 27, L_s and ρ_{sh} depend on the square root of R_i. Because a larger value of R_i leads to a larger L_s and a smaller ρ_{sh}, the attenuation of the effective current due to the spine becomes severe for large R_i. If we assume $R_i = 1{,}000\ \Omega$cm, which is 10 times higher than usual, this leads to $\bar{L}_s = 0.028$ and $\bar{\rho}_{sh} = 11.1$. As we have seen in section entitled Quantitative Assessment of the Straightforward Attentuation Effect of the Dendritic Spine, these values still produce only a negligible effect.

Second, we approximate $H(p)$ by $G(p)$ on the assumption that the diameter of the spine stalk is very small compared with that of the parent dendrite. If a very thick spine stalk is attached to a very thin parent dendrite, this assumption does not hold true and $G(p)$ might be quite different from $H(p)$. To emphasize the possible difference between $G(p)$ and $H(p)$, we take an example of the largest spine ($a_s = 0.15\ \mu$m, $l_s = 3\ \mu$m, $S_h = 13\ \mu m^2$) and a thin parent dendrite ($a_d = 0.3\ \mu$m). To complete overestimation of the difference, we assume that $F(p) = 1$. For these values of parameter we obtain $H(0) = 0.969$ and $G(0) = 0.999$. Recall that $H(0)$ or $G(0)$ is equal to the portion of injected electrical charge that reaches the parent dendrite. So, actually 3.1% of the synaptic current does not reach the parent dendrite, but our assumption makes it 0.1%. Hence, our approximation is not accurate in this specific example. However, both $H(0)$ and $G(0)$ are sufficiently close to 1 and the approximation is not so bad in this sense. Our conclusion that the spine does not produce an effective straightforward attenuation effect still remains valid.

Our major conclusions in this paper are as follows. (*a*) The isolation effect of the spine on the synapse from the electrical effects of neighboring synapse is negligible. (*b*) When the synaptic resistance is large compared with the spine stem resistance, a morphological change of the spine, if it were to take place, would lead to only negligible changes in the postsynaptic potential. Moreover, we suggested the following possibility. (*c*) On the other hand, when the synaptic resistance is comparable with the input impedance of the spine stalk, a morphological change of the spine may induce the effective change of the postsynaptic potential by changing the synaptic input current itself.

The second conclusion is in good agreement with the results of Jack et al. (1975). At first sight, it appears in sharp contrast to the results of Rall (1974, 1978). However, Rall implicitly assumed that the synaptic resistance is comparable with the spine stem resistance. Hence, our third conclusion is in agreement with his results. In subsequent papers we hope to study the change of the synaptic current based on the values of synaptic conductance and the three-dimensional morphology of the neuron, which are obtained experimentally.

APPENDIX A

Butz and Cowan's Theorem

Butz and Cowan (1974) developed the graphical calculus that generates analytic solutions for membrane potential at any point on the dendritic tree of neurons with arbitrary dendritic geometries in response to synaptic current inputs at any point. Using this mathematical technique, we investigate the transient electrical behavior of dendritic spines with end bulbs. We briefly illustrate their results in this Appendix.

Theorem (Butz and Cowan, 1974). On a dendritic tree of arbitrary geometry, the membrane potential transform, $V(x, p)$, at a point x on any branch due to a current source transform, $I_{syn}(p)$, at a point y on the same or any other branch of the tree is a quotient whose numerator and denominator are expressions involving sums and products of the hyperbolic trigonometric functions sinh and cosh. One can then develop a geometric notation whereby the denominator is represented by a graph structure topologically isomorphic to the physical dendritic tree and the numerator is given by the following deletion rule: For any dendritic tree, delete the direct path from the point x at which the membrane potential is desired to the location y of the current source. This deletion dismembers the dendritic tree into disjoint connected sets. Then (*a*) the geometric notation of the numerator simply corresponds to a product of structures topologically isomorphic to the resulting disjoint sets of connected dendritic branches, and (*b*) for each bifurcation point deleted in the tree, there is a corresponding algebraic product of three characteristic impedances in the numerator. If the bifurcation point is the junction of branches labeled k, l, m, the product is $Z_k Z_l Z_m$.

They then gave the explicit expressions of the geometric notation for the case of arbitrary boundary conditions. Let $B(p)$ be the terminal impedance of one end ($x = 0$) of a dendritic branch, representing the following boundary condition

$$V(0, p) = -B(p)I(0, p). \tag{A1}$$

The graphical, geometric notation, denoted by the value in the square brackets [], is defined for one branch case as follows

$$\left[\textcircled{B} \overset{x}{\text{—}} \right] = Z \cdot \sinh \gamma x + B \cdot \cosh \gamma x. \tag{A2}$$

One end of the cylinder satisfies the boundary condition (Eq. A1). The other end of the cylinder is killed, that is, $v(x, t) = 0$. In other words, terminal impedance of this end is 0. A graph operation called conjugacy, which is denoted by an asterisk, is simply the interchange of sinh's and cosh's

$$\left[\textcircled{B} \overset{x}{\text{—}} \right]^* = Z \cdot \cosh \gamma x + B \cdot \sinh \gamma x. \tag{A3}$$

The geometric notation is defined inductively using the conjugacy

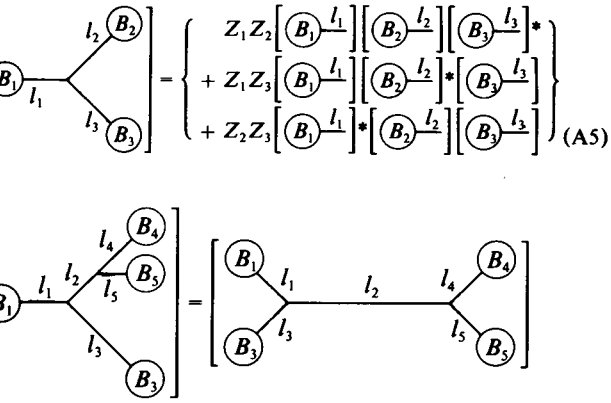

(A4)

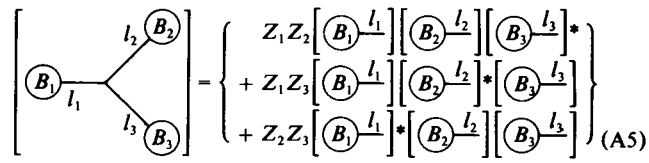

(A5)

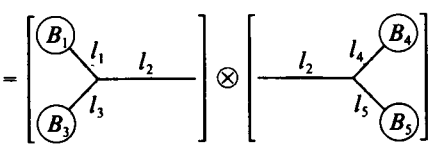

(A6)

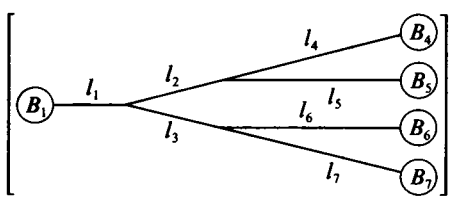

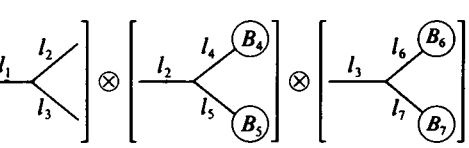

(A7)

This graphical notation is defined inductively for higher order branching by similar decomposition using the commutative operation ⊗ as in Eqs. A6 and A7. The operator ⊗ represents multiplication in the ordinary sense when the corresponding analytic formulae (Eq. A5) are substituted, except for terms involving the common branches (that is, l_2 in Eq. A6 and l_2 and l_3 in Eq. A7) for which the following "parity" rule applies

$$Z_k \sinh \gamma_k l_k \otimes Z_k \sinh \gamma_k l_k \rightarrow Z_k \sinh \gamma_k l_k$$
$$Z_k \cosh \gamma_k l_k \otimes Z_k \cosh \gamma_k l_k \rightarrow Z_k \sinh \gamma_k l_k$$
$$Z_k \cosh \gamma_k l_k \otimes Z_k \sinh \gamma_k l_k \rightarrow Z_k \cosh \gamma_k l_k$$
$$k = 2 \text{ in Eq. A6,}$$
$$k = 2, 3 \text{ in Eq. A7.} \qquad \text{(A8)}$$

APPENDIX B

Derivation of Eq. 10

The postsynaptic potential transform caused by the synapse on the spine (see Fig. 1) is derived by Butz and Cowan's theorem (1974) to be

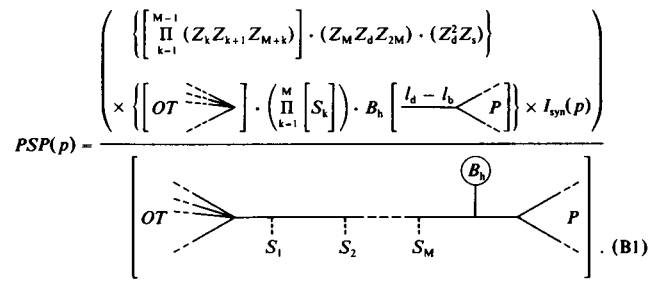

(B1)

We define $K(p)$ as follows

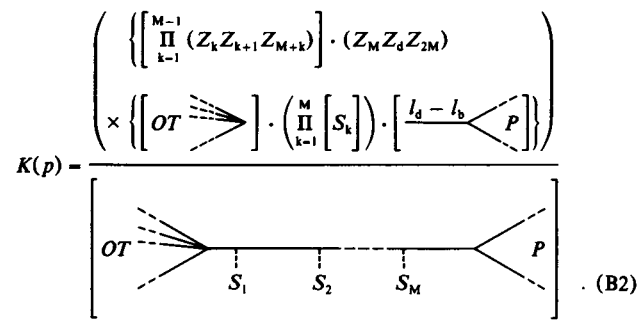

(B2)

From Butz and Cowan's theorem it is easy to see that $K(p)$ is the Laplace transform of voltage transient, $k(t)$, at the soma of the neuron without the spine in response to a current pulse injected at BP. $H(p)$ is defined as follows

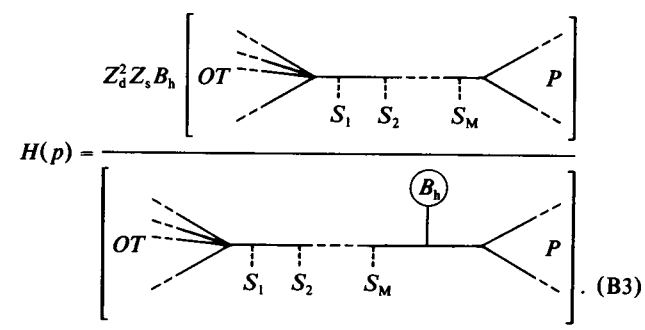

(B3)

From Eqs. B1–B3, the following decomposition of $PSP(p)$ is trivial

$$PSP(p) = K(p) \cdot H(p) \cdot I_{syn}(p). \qquad \text{(B4)}$$

This is the required result. It is also easy to prove that $H(p) \cdot I_{syn}(p)$ is the Laplace transform of the effective current, $i_{eff}(t)$, which reaches the parent dendrite (see Fig. 2).

APPENDIX C

Explicit Expression of $H(p)$

$H(p)$ of Eq. B3 can be rewritten as follows

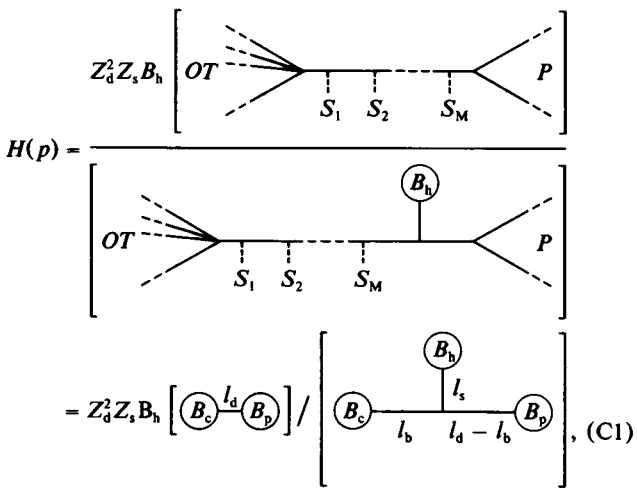

, (C1)

where $B_c(p)$ and $B_p(p)$ represent terminal impedances of the parent dendrite at the proximal and the peripheral ends. That is, $B_c(p)$ is an input impedance of the dendritic tree proximal to the parent dendrite at its proximal end. Similarly $B_p(p)$ is an input impedance of the dendritic subtree P at the peripheral end of the parent dendrite. Eq. C1 is transformed using Eqs. A4 and A5

$$H(p) = Z_d Z_s B_h \Big/ \Big\{ Z_s Z_d \left[B_h \xrightarrow{l_s} \right] + Z_d^2 \Big(\left[B_c \xrightarrow{l_b} \right] \times \left[B_p \xrightarrow{l_d - l_b} \right] \times \left[B_h \xrightarrow{l_s} \right]^* \Big) \Big/ \Big(\left[B_c \xrightarrow{l_b} \right] \times \left[B_p \xrightarrow{l_d - l_b} \right]^* + \left[B_c \xrightarrow{l_b} \right]^* \left[B_p \xrightarrow{l_d - l_b} \right] \Big) \Big\} = 1 \Big/ \Big[(Z_s/B_h) \sinh \gamma_s l_s + \cosh \gamma_s l_s + (Z_d/B_h) F(p) \cosh \gamma_s l_s + (Z_d/Z_s) F(p) \sinh \gamma_s l_s \Big], \tag{C1a}$$

where

$$F(p) = \left[B_c \xrightarrow{l_b} \right] \left[B_p \xrightarrow{l_d - l_b} \right] \Big/ \Big(\left[B_c \xrightarrow{l_b} \right] \left[B_p \xrightarrow{l_d - l_b} \right]^* + \left[B_c \xrightarrow{l_b} \right]^* \left[B_p \xrightarrow{l_d - l_b} \right] \Big). \tag{C2}$$

Substituting Eqs. 12 and 13 into Eq. C1a, we obtain the following equation

$$1/H(p) = \cosh \gamma_s l_s + (q/\rho_{sh}) \sinh \gamma_s l_s + (a_s/a_d)^{3/2} F(p) \cdot [\sinh \gamma_s l_s + (q/\rho_{sh}) \cosh \gamma_s l_s]. \tag{C3}$$

This is exactly Eq. 18.

APPENDIX D

In this Appendix, we prove that $F(p)$ is at most on the order of 1 [$F(p) \sim O(1)$] assuming two points that are usual for ordinary configurations of neurons. The first assumption is that the diameter of the kth branch is larger than that of the (k + 1) branch. The second is that the input resistance of the neuron at the soma is at most on the order of $10^7\Omega$. The latter is true for red nucleus neurons, pyramidal tract neurons, and hippocampal neurons that have dendritic spines (Tsukahara et al., 1975; Takahashi, 1965; Spencer and Kandel, 1961).

We can rewrite Eq. C2 using definitions of geometric notation in Eqs. A2 and A3

$$F(p) = \frac{\left\{ \begin{array}{l} Z_d^2 [\cosh \gamma_d l_d - \cosh \gamma_d (2l_b - l_d)] \\ \quad + Z_d B_p [\sinh \gamma_d l_d + \sinh \gamma_d (2l_b + l_d)] \\ \quad + Z_d B_c [\sinh \gamma_d l_d + \sinh \gamma_d (2l_b + l_d)] \\ \quad + B_c B_p [\cosh \gamma_d l_d + \cosh \gamma_d (2l_b - l_d)] \end{array} \right\}}{Z_d^2 \sinh \gamma_d l_d + Z_d B_p \cosh \gamma_d l_d + Z_d B_c \cosh \gamma_d l_d + B_c B_p \sinh \gamma_d l_d}. \tag{D1}$$

The following inequalities hold because $0 < l_b < l_d$

$$\begin{aligned} 0 &< \cosh \gamma_d l_d - \cosh \gamma_d (2l_b - l_d) < \cosh \gamma_d l_d, \\ 0 &< \sinh \gamma_d l_d + \sinh \gamma_d (2l_b - l_d) < 2 \sinh \gamma_d l_d, \\ 0 &< \sinh \gamma_d l_d - \sinh \gamma_d (2l_b - l_d) < 2 \sinh \gamma_d l_d, \\ 0 &< \cosh \gamma_d l_d + \cosh \gamma_d (2l_b - l_d) < 2 \cosh \gamma_d l_d. \end{aligned} \tag{D2}$$

Since $Z_d(p)$, $B_p(p)$, and $B_c(p)$ are non-negative for all $p \geq 0$, we obtain

$$F(p) < \frac{(Z_d^2 + B_c B_p) + (Z_d B_p + Z_d B_c) \tanh \gamma_d l_d}{(Z_d B_p + Z_d B_c) + (Z_d^2 + B_c B_p) \tanh \gamma_d l_d}. \tag{D3}$$

From this inequality we find that $F(p)$ gets much larger than 1 only when the following four conditions are satisfied

$$\begin{aligned} p &\ll 1, \\ l_d &\ll 1, \\ B_c &\gg Z_d, \\ B_p &\gg Z_d. \end{aligned} \tag{D4}$$

On the first assumption of this Appendix, we obtain the following evaluation for $B_c(0)$

$$B_c(0) \leq Z_d(0) \frac{Z_d(0) \tanh L + \hat{R}_{soma}}{Z_d(0) + \hat{R}_{soma} \tanh L}, \tag{D5}$$

where L is electrotonic distance between the proximal end of the parent dendrite and the soma, and $\hat{R}_{soma}$ is the input resistance at the soma of the neuron without the subtree, which contains the spine. The third condition of Eq. D4 and the inequality of Eq. D5 together imply $L \ll 1$. This and the second condition of Eq. D4 $L_d \ll 1$ lead

$$1/R_{in} \sim 1/B_c(0) + 1/B_p(0). \tag{D6}$$

Because $R_{in} < Z_d(0)$, from the second assumption made at the beginning of this appendix, we find that

$$B_p(0) \sim R_{in} < Z_d(0). \tag{D7}$$

Hence, the fourth condition of Eq. D4 is not satisfied. Consequently, we conclude that $F(p)$ is on the order of 1.

APPENDIX E

Here we calculate the inverse Laplace transform $g(t)$ of $G(p)$, which is given in Eq. 25. To obtain $g(t)$, $G(p)$ itself must be arranged into a form for which the inverse transform may be found. Eq. 25 may be rewritten

$$G(p) = 2\rho_{sh} \sum_{n=0}^{\infty} \frac{(\sqrt{\tau p + 1} - \rho_{sh})^n}{(\sqrt{\tau p + 1} + \rho_{sh})^{n+1}} e^{-(2n+1)L_s\sqrt{\tau p+1}}. \quad \text{(E1)}$$

From Jack and Redman (1971, p. 349, Eqs. A13–A16), we get the following transform pair

$$U(p) = \frac{(\sqrt{p} - \rho_{sh})^n}{(\sqrt{p} + \rho_{sh})^{n+1}} e^{-Z\sqrt{p}}$$

$$u(t) = \frac{1}{\sqrt{2\pi}\,\rho_{sh} t} e^{-Z^2/(4t)} \exp(k^2/4) \sum_{r=0}^{n}$$

$$\cdot \frac{(-n)_r}{r!} 2^{3r/2} \rho_{sh}^{r+1} t^{r/2}$$

$$\times [(r+1)\sqrt{2t}\, D_{-r-2}(k) + Z D_{-r-1}(k)], \quad \text{(E2)}$$

where $k = \sqrt{2}\,\{\rho_{sh}\sqrt{t} + [(2n+1)L/2\sqrt{t}]\}$ and $(-n)_r = (-n)(-n+1)(-n+2)\ldots(-n+r-1)$. For the transform pair $U(p) \leftrightarrow u(t)$, it is well known that $U(p+1) \leftrightarrow \exp(-t)u(t)$ and $U(\tau p + 1) \leftrightarrow (1/\tau) \cdot \exp(-t/\tau) \cdot u(t/\tau)$ hold true. Hence we obtain Eq. 26.

Received for publication 14 December 1982 and in final form 16 April 1984.

REFERENCES

Barrett, J. N., and W. E. Crill. 1974. Influences of dendritic location and membrane properties on the effectiveness of synapses on cat motoneurones. *J. Physiol. (Lond.)*. 293:325–345.

Butz, E. G., and J. D. Cowan. 1974. Transient potentials in dendritic systems of arbitrary geometry. *Biophys. J.* 14:661–690.

Chang, H. T. 1952. Cortical neurons with particular reference to the apical dendrites. *Cold Spring Harbor Symp. Quant. Biol.* 17:189–202.

Crick, F. 1982. Do dendritic spines twitch? *Trends Neurosci.* 5:44–46.

Fifkova, E., and A. van Harreveld. 1977. Long-lasting morphological changes in dendritic spines of dentate granular cells following stimulation of the entorhinal area. *J. Neurocytol.* 6:211–230.

Horwitz, B. 1981. An analytical method for investigating transient potentials in neurons with branching dendritic trees. *Biophys. J.* 36: 155–192.

Jack, J. J. B., D. Noble, and R. W. Tsien. 1975. Electric Current Flow in Excitable Cells. Clarendon Press, Oxford. 502.

Jack, J. J. B., and S. J. Redman. 1971. An electrical description of the motoneurone, and its application to the analysis of synaptic potentials. *J. Physiol. (Lond.)*. 215:321–352.

Jones, E. G., and T. P. S. Powell. 1969. Morphological variations in the dendritic spines of the neocortex. *J. Cell Sci.* 5:509–529.

Katsumaru, H., F. Murakami, and N. Tsukahara. 1982. Actin filaments in dendritic spines of red nucleus neurons demonstrated by immunoferritin localization and heavy meromyosin binding. *Biomed. Res.* 3: 337–340.

Kawato, M., and N. Tsukahara. 1983. Theoretical study on electrical properties of dendritic spines. *J. Theor. Biol.* 103:507–522.

Lee, K. S., F. Schottler, M. Oliver, and G. Lynch. 1980. Brief bursts of high-frequency stimulation produce two types of structural change in rat hippocampus. *J. Neurophysiol. (Bethesda)*. 44:247–258.

Peters, A., and I. R. Kaiserman-Abramof. 1970. The small pyramidal neuron of the rat cerebral cortex. The perikaryon, dendrites and spines. *Am. J. Anat.* 127:321–356.

Rall, W. 1959. Branching dendritic trees and motoneuron membrane resistivity. *Exp. Neurol.* 1:491–527.

Rall, W. 1970. Cable properties of dendrites and effects of synaptic location. *In* Excitatory Synaptic Mechanisms. P. Andersen and J. K. S. Jansen, editors. Universitetsforlaget, Oslo. 175–187.

Rall, W. 1974. Dendritic spines, synaptic potency and neuronal plasticity. *In* Cellular Mechanisms Subserving Changes in Neuronal Activity. C. D. Woody, K. A. Brown, T. J. Crow Jr., and J. D. Knispel, editors. University of California, Los Angeles. 13–21.

Rall, W. 1978. Dendritic spines and synaptic potency. *In* Studies in Neurophysiology. R. Porter, editor. Cambridge University Press, London. 203–209.

Rall, W., and J. Rinzel. 1973. Branch input resistance and steady attenuation for input to one branch of a dendritic neuron model. *Biophys. J.* 13:648–688.

Rinzel, J., and W. Rall. 1974. Transient response in a dendritic neuron model for current injected at one branch. *Biophys. J.* 14:759–790.

Spencer, W. A., and E. R. Kandel. 1961. Electrophysiology of hippocampal neurons. III. Firing level and time constant. *J. Neurophysiol. (Bethesda)*. 24:260–271.

Takahashi, K. 1965. Slow and fast groups of pyramidal tract cells and their respective membrane properties. *J. Neurophysiol. (Bethesda)*. 28:908–924.

Tsukahara, N., H. Hultborn, F. Murakami, and Y. Fujito. 1975. Electrophysiological study of formation of new synapses and collateral sprouting in red nucleus neurons after partial denervation. *J. Neurophysiol. (Bethesda)*. 38:1359–1372.

Tsukahara, N., and K. Kosaka. 1968. The mode of cerebral excitation of red nucleus neurons. *Exp. Brain Res.* 5:102–117.

Tsukahara, N., F. Murakami, and H. Hultborn. 1975. Electrical constants of neurons of the red nucleus. *Exp. Brain Res.* 23:49–64.

Tsukahara, N., and Y. Oda. 1981. Appearance of new synaptic potentials at cortico-rubral synapses after the establishment of classical conditioning. *Proc. Jpn. Acad.* 57:398–401.

Valverde, F. 1967. Apical dendritic spines of the visual cortex and light deprivation in the mouse. *Exp. Brain Res.* 3:337–352.

Wilson, C. J. 1982. A cable model of axo-spinous synaptic activation of the spiny projection neuron of mammalian neostriatum. *Soc. Neurosci. Symp.* 8:491. (Abstr.)